



Published in final edited form as:

Int J Pharm. 2015 June 20; 487(0): 91–100. doi:10.1016/j.ijpharm.2015.04.032.

Microheterogeneity in Frozen Protein Solutions

Alan Twomey¹, Kosaku Kurata², Yutaka Nagare², Hiroshi Takamatsu², and Alptekin Aksan^{1,*}

¹Biostabilization Laboratory, Mechanical Engineering Department, College of Science and Engineering, University of Minnesota, Minneapolis, MN 55455

²Heat and Mass Transfer Laboratory, Mechanical Engineering Department, Kyushu University, Fukuoka, Japan

Abstract

In frozen and lyophilized systems, the biological to be stabilized (e.g. therapeutic protein, biomarker, drug-delivery vesicle) and the cryo-/lyoprotectant should be co-localized for successful stabilization. During freezing and drying, many factors cause physical separation of the biological from the cryo-/lyoprotectant, called microheterogeneity (**MH**), which may result in poor stabilization efficiency. We have developed a novel technique that utilized confocal Raman microspectroscopy in combination with counter-gradient freezing to evaluate the effect of a wide range of freezing temperatures ($-20 < T_F < 0^\circ\text{C}$) on the **MH** generated within a frozen formulation in only a few experiments. The freezing experiments conducted with a model system (albumin and trehalose) showed the presence of different degrees of **MH** in the freeze-concentrated liquid (**FCL**) in all solutions tested. Mainly, albumin tended to accumulate near the ice interface, where it was physically separated from the cryoprotectant. In frozen 10 wt% trehalose solutions, heterogeneity in **FCL** was relatively low at any T_F . In frozen 20 wt% trehalose solutions, the optimum albumin to trehalose ratio in the **FCL** can only be ensured if the solution was frozen within a narrow range of temperatures ($-16 < T_F < -10^\circ\text{C}$). In the 30 wt% trehalose solutions, freezing within a much more narrow range ($-12 < T_F < -10^\circ\text{C}$) was needed to ensure a fairly homogeneous **FCL**. The method developed here will be helpful for the development of uniformly frozen and stable formulations and freezing protocols for biological as **MH** is presumed to directly impact stability.

1. INTRODUCTION

Pharmaceuticals such as therapeutic proteins, vaccines, and small molecule drugs as well as biospecimens such as serum, plasma, and urine have to be frozen, dried and/or lyophilized

© 2015 Published by Elsevier B.V.

*Corresponding Author. Alptekin Aksan, Ph.D., Associate Professor, Mechanical Engineering Department, & BioTechnology Institute, University of Minnesota, 241 Mechanical Engineering, 111 Church St SE, Minneapolis, MN 55455, aaksan@umn.edu, Phone: (612)626-6618.

Publisher's Disclaimer: This is a PDF file of an unedited manuscript that has been accepted for publication. As a service to our customers we are providing this early version of the manuscript. The manuscript will undergo copyediting, typesetting, and review of the resulting proof before it is published in its final citable form. Please note that during the production process errors may be discovered which could affect the content, and all legal disclaimers that apply to the journal pertain.

for long-term stabilization and storage (Aksan and Toner, 2006; Carpenter and Chang, 1996; Chang et al., 2005; Crowe et al., 1988; Hubel et al., 2011; Peakman and Elliott, 2008; Riegman et al., 2008). However, freezing and drying induce significant thermal, osmotic, mechanical, physical and chemical stresses. These stresses can cause proteins and enzymes to get irreversibly damaged by denaturation, aggregation or crystallization (Bhatnagar et al., 2007; Carpenter and Crowe, 1989; Carpenter et al., 1990; Chang et al., 2005; Crowe et al., 1990; Pikal, 1994; Ragoonanan and Aksan, 2007; Randolph and Carpenter, 2007; Tang and Pikal, 2005). Furthermore, during storage, certain pharmaceuticals have been shown to continue to lose activity and efficacy (Bhatnagar et al., 2007; Eckhardt et al., 1991a; McLerran et al., 2008c) and even develop immunogenic characteristics (Fradkin et al., 2009) causing undesired side-effects upon administration to a patient (Rathore and Rajan, 2008) and an inferior therapeutic outcome. Similarly, when biospecimens are frozen or desiccated, the molecular biomarkers they contain (enzymes, proteins, lipids, DNA, RNA, etc.) can be damaged by a variety of chemical and physical mechanisms (Hubel et al., 2011; Zimmermann et al., 2008). This reduces their diagnostic and clinical utility, and negatively impacts the quality of the analytic studies and the clinical research that utilize stored biospecimens (McLerran et al., 2008a; McLerran et al., 2008b; McLerran et al., 2008c).

To protect the biologicals against freezing, drying and storage-induced stresses, cryo-/lyoprotectant chemicals (e.g. trehalose, sucrose, glycerol, amino acids, dimethylsulfoxide) are often added to the pharmaceutical formulation or to the biospecimen (Carpenter et al., 1990; Kawai and Suzuki, 2007; Tang and Pikal, 2004). Independent of the mechanism of protection they offer, cryo-/lyoprotectants should be co-localized with the biological to ensure maximum protective action (Dong et al., 2009a) (Piedmonte et al., 2007; Twomey et al., 2013). However, the thermal and osmotic gradients and the mechanical stresses induced during the freezing and drying processes may cause physical separation of the biological from the cryo-/lyoprotectant (Dong et al., 2009b; Padilla and Pikal, 2011; Schwegman et al., 2009). These stresses also may cause spatial variations in the distributions of other excipients (such as the buffering ions and the bulking agents) within the frozen or the dried medium (Cavatur et al., 2002; Sundaramurthi et al., 2009).

Microheterogeneity (**MH**) is defined as the spatial variations and non-uniformities in the composition and thermodynamic phase of a system (Dong et al., 2009a; Ragoonanan and Aksan, 2008; Twomey et al., 2013). Presence of **MH** in desiccated, frozen (Izutsu and Kojima, 2000) and lyophilized protein solutions (Heller et al., 1999b) has previously been detected using thermogravimetric and calorimetric analyses (Heller et al., 1999a; Jovanovic et al., 2006; Murase and Franks, 1989; Randolph, 1997; Shalaev and Franks, 1996; Shalaev and Kanev, 1994; Suzuki and Franks, 1993), X-Ray diffractometry (Cavatur and Suryanarayanan, 1998), and Infrared (IR) spectroscopy (Heller et al., 1996; Jovanovic et al., 2006; Remmele and Stushnoff, 1994). The ultrastructural variations in the frozen and desiccated media have also been visualized using transmitted light, freeze-fracture (FF) and scanning electron microscopy (SEM) techniques (Heller et al., 1997; Murase et al., 1991; Uchida et al., 2012). Even though **MH** was detected in bulk samples and was visualized (by microscopy) in these earlier studies, it was not until very recently that it was possible to quantify it by directly measuring the distribution of the protein and the cryo-/lyoprotectant

within different regions in desiccated (Ragoonanan and Aksan, 2008), frozen (Dong et al., 2009a; Twomey et al., 2013), and lyophilized media (Padilla and Pikal, 2011). These recent studies showed that **MH** is very sensitive to the chemical composition of the medium and varies very significantly with the freezing and drying conditions applied. It has not yet been possible to determine the exact role **MH** plays on storage stability. This was mainly because these studies have been burdened by the enormous number of experiments required where the formulation composition, freezing temperature, cooling rate and the drying conditions are to be varied in a systematic manner.

In this communication, we introduce a new method called Counter-gradient Freezing Raman Microspectroscopy (**CFRM**), which combines Confocal Raman Microspectroscopy (**CRM**) (Dong et al., 2009a) with counter-gradient directional freezing, to map and quantify the distribution of **MH** in a model protein-cryoprotective agent solution containing albumin and trehalose (Figure 1). By imposing a linear thermal gradient on the (initially supercooled) model solution, the effect of ice growth temperature could then be systematically explored, enabling testing of a very large combination of freezing conditions with a few experiments. Our results mainly showed that different levels of **MH** existed in almost all frozen specimens and it increased with increasing trehalose concentration in the solution. These findings are very novel and are expected to have important implications in cryopreservation/lyophilization formulation science and technology development. It is not yet known how **MH** in the frozen medium directly affects the stability of the frozen biologicals but extensive work is currently being conducted by our group (and others) to understand and establish its effects.

2. MATERIALS AND METHODS

In this communication, a new method called Counter-gradient Freezing Raman Microspectroscopy (**CFRM**) was developed and characterized. A confocal Raman microscope (Nanophoton, Osaka, Japan) was connected to an in-house directional freezing stage to induce ice growth against a linear temperature gradient imposed on a liquid sample (Figure 1). This generated a frozen sample where the freezing history changed spatially from one location to another. Spectral analysis of the frozen medium was then conducted to determine the relative concentrations of the model protein and the cryoprotectant agent as a function of spatial location (corresponding to a different freezing history) in the medium. Therefore **CFRM** enabled determination of the changes in the degree of co-localization of the model protein and the lyoprotectant agent (i.e. **MH**) for a wide range of freezing temperatures, in a single experiment.

Calibrations and experiments were performed using solutions that were prepared gravimetrically with powder trehalose dihydrate (97% Purity, Wako, Osaka, Japan), bovine serum albumin (98% Purity, Sigma-Aldrich, St. Louis, MO) and 1× Dulbecco's phosphate buffered saline solution (14190-144, Invitrogen Corporation, Burlington, Ontario, Canada). Experiments were conducted with frozen aqueous solutions prepared at a wide range of trehalose (10–35 wt%) and albumin concentrations (2–12 wt%).

The in-house directional freezing stage was composed of a high temperature block (a copper block heated by resistance heaters) and a low temperature block separated by a small gap. The low temperature copper block was cooled by circulating the bleed-off from a liquid nitrogen tank ($T = -120\text{ }^{\circ}\text{C}$) and simultaneously heated by resistance heaters to control its temperature. The resistance heaters were connected to temperature controllers that monitored the thermocouples placed on the high and low temperature blocks. The two copper blocks were physically separated by an adjustable gap, d (Figure 1). A microchannel (containing the sample solution to be tested) was then placed forming a bridge between the two blocks. The microchannel was 1 mm wide and 10 mm long, and was machined in a 50 μm thick silicone film that was then sandwiched between two quartz windows. The length of the microchannel was set at 10 mm (approximately, 4 times the size of the gap it bridges) to ensure that the sample was in good thermal contact with the high and low temperature blocks while bridging the gap between them. The width of the microchannel was set at 1 mm to minimize the capillary and the edge effects on ice propagation. The small thickness of the microchannel (50 μm) ensured that natural convection effects within the solution (before freezing) was negligible, the solution could be assumed to be isothermal in the vertical direction, ice propagation was mainly in one direction, and the Raman signal/noise ratio was high with reasonably low amount of heat generation (induced by Raman laser heating). This setup thus imposed a linear temperature gradient on the sample solution spanning across the gap (Figure 2B) while enabling optical and spectroscopic access (Figure 2A). The microchannel was connected to two large reservoirs at each end. The temperatures of the reservoirs were kept constant as they were directly over and in contact with their respective copper blocks.

The confocal Raman microscope was equipped with a 100 \times Nikon air objective (NA 0.90) and a 532 nm AR-ion laser operating at a maximum power of 12 mW for excitation and a CCD detector electrically cooled to -70°C . Spatial resolution was 350 nm in the x-y plane and the depth resolution was 1000 nm. Each Raman scan was conducted over 8000 locations within a $4\text{ }\mu\text{m} \times 83\text{ }\mu\text{m}$ region of the sample (Figure 2A). Each spectrum had a spectral resolution of 6 cm^{-1} in the $3900\text{--}70\text{ cm}^{-1}$ wavenumber range with an integration time of 0.05 s per location to minimize local heating. To improve the signal to noise ratio, the collected spectra were spatially averaged over two pixels in each direction, thereby reducing the number of spectra per scan from 8000 to 2000. The spectra were then processed by applying 15 point Savitsky-Golay smoothing and analyzed using CytoSpec software (Boston, MA) and Matlab (MathWorks, Natick, MA).

2.1. Spectral Calibration Experiments

For calibration purposes, the changes in the Raman spectra with trehalose and albumin concentration and temperature were explored. Solutions of trehalose and albumin were supercooled at a rate of $10^{\circ}\text{C}/\text{min}$ down to -20°C without ice nucleation. Cooling was paused to collect spectra at 0, -5 , -10 , -15 , and -20°C . See Table 1 for a list of solutions used in calibration.

2.2. Directional Freezing Experiments

CFRM experiments were performed with combinations of 10–30 wt% trehalose and 2–4 wt % albumin (Table 2). Each freezing experiment involved introducing 3 μL of the experimental solution into the microchannel through the fluid reservoirs at both ends. The microchannel containing the experimental solution was then positioned across the two temperature-controlled copper blocks (initially kept at room temperature). The blocks were heated/cooled slowly until they reached their pre-set temperatures of 16°C and –20°C. Note that the block temperatures were continuously measured and found to remain within $\pm 2^\circ\text{C}$ of the set temperatures throughout the experiments. This setup generated a temperature gradient, dT/dx , along the microchannel, which was linear in the region of interest (where Raman spectra were collected) (Figure 2B). The temperature measurements in the gap (Figure 2B) were conducted by embedding 0.25 mm diameter thermocouples at a spacing of 1 mm in a microchannel that contained deionized water.

Once the temperature gradient across the liquid sample was steadied, ice was nucleated at the low temperature reservoir by injecting a small amount of silver iodide into the experimental solution (Figure 1). This caused the ice front to rapidly propagate along the microchannel (towards the high temperature reservoir) until it reached a certain location along the microchannel. Naturally, this location corresponded to the melting temperature of the experimental solution used. Figure 2C shows the measured ice propagation speed in different experimental solutions. Once ice propagation stopped, transmitted light images and confocal Raman spectral maps were collected at 0.5 mm increments (Figures 1 & 2A), starting from the low temperature side of the gap and moving towards the high temperature side, stopping at the ice interface. This generated Raman maps of the solution frozen with ice propagating at different temperatures (see insert in Figure 2A for a typical Raman map), which were later analyzed to determine the concentrations of ice, trehalose and albumin.

2. RESULTS & DISCUSSION

The interaction between the macromolecules in a solution and an advancing ice front is of particular interest in stabilization of pharmaceutical biologicals and biospecimens by freezing and lyophilization. It is reported that the structures of certain proteins and enzymes change drastically, and sometimes irreversibly, at the ice interface (Hew and Yang, 1992; Strambini and Gabellieri, 1996; Strambini and Gonnelli, 2007). Some of these structural changes result in aggregation of the macromolecules, a condition that may even persist after thawing (Bhatnagar et al., 2007; Eckhardt et al., 1991b; Kerwin et al., 1998). This is one major reason for the immune reaction to injected therapeutic formulations and also is a source of product loss during manufacturing in pharmaceutical industry. In biospecimen preservation field, ice and cold-induced denaturation and aggregation phenomena cause significant loss of the molecular information that the biospecimens contain (Hubel et al., 2011). As a result, it is of great importance to identify the freezing conditions (and the formulations) that would minimize the potentially harmful interactions between the biologicals to be stabilized and the ice phase.

Theoretically, a growing ice crystal excludes solutes (Cuffey et al., 1999; Hobbs, 1974), which accumulate in a freeze-concentrated liquid (**FCL**) phase (Butler, 2002; Hobbs, 1974).

However, freezing is a complex kinetic phenomenon governed by thermal, physical and chemical factors. An advancing ice front may move very slowly (in the order of $\mu\text{m/s}$) and stay planar, rejecting most, if not all of the solutes (Butler, 2002; Nagashima and Furukawa, 1997). This is mainly possible since the partition coefficient (between the solid and liquid phases) for most solutes is very low (Korber, 1988). However, an advancing planar ice interface is inherently unstable (Langer, 1980). With increasing propagation speed, solution viscosity, cooling rate, and/or due to the presence of impurities within the medium, the planar interface may rapidly destabilize, inducing cellular or dendritic ice growth (Korber, 1988; Korber et al., 1983; Langer, 1980). In cellular/dendritic ice growth regimes, the growing ice dendrites engulf and entrap the solutes within the growing ice phase in small, isolated channels or lacunae of supercooled solution (Dong et al., 2009b; Korber, 1988; Korber et al., 1983; Lipp and Körber, 1993). This phenomena stabilizes the solute concentration accumulating in front of the moving ice interface (Nagashima and Furukawa, 1997), reaching a steady state at approximately 25% higher than the concentration of the initial solution (Figure 3 in Nagashima & Furukawa, 1997 (Nagashima and Furukawa, 1997)). Cellular/dendritic ice growth is very common in freezing of pharmaceutical solutions and liquid biospecimens and therefore was the focus of the study conducted here.

In this study, albumin was chosen as the model protein as it is the most abundant protein found in the human blood (Klajnert and Bryszewska, 2002; Shen et al., 2004). It facilitates the transport of thyroid and steroid hormones (Pardridge, 1987; Pardridge and Mietus, 1979), fatty acids (Bhattacharya et al., 2000), and regulates the oncotic pressure in the capillaries (Gekle, 2005). Furthermore, ensuring its stability in frozen biospecimens is very important since it is used as a biomarker for renal and cardiovascular diseases (Basi and Lewis, 2006). Aggregation of albumin in biospecimens could result in errors in the diagnosis of not only these conditions but also many others since albumin aggregates are known to act as “sinks” for other low abundance biomarkers, resulting in false negatives. As the model cryoprotective agent, we used trehalose, which is a disaccharide widely used in preservation of cells, tissues and pharmaceuticals thanks to its ability to protect macromolecules from freeze and desiccation-induced damage (Leslie et al., 1995; Lins et al., 2004; Wolkers et al., 2001).

3.1. Spectral Calibration and Analysis

Raman spectroscopy was used to map the distribution of trehalose and albumin (the model protein to be preserved and the cryo-/lyoprotectant agent) in directionally frozen solutions to determine how the ice propagation temperature affected their relative distribution in the frozen medium, i.e. **MH**. Any cryo-/lyoprotective agent can only protect the macromolecule against freezing or desiccation damage if it is physically very close to it (co-localization). In a freezing solution very significant thermal, osmotic and chemical gradients form, affecting the molecular mobility of the solutes and their affinity/susceptibility to an advancing ice phase greatly. For example, during freezing an excipient may precipitate out or aggregate, radically changing its concentration in the **FCL** phase post freezing (resulting in **MH**). Therefore, in a medium with a significant degree of **MH** - even though they may be present in large numbers - cryo-/lyoprotective agents might be physically separated from the macromolecule to be stabilized. In the absence of the protective agent, macromolecule can

easily be exposed to the stresses at the ice interface (Dong et al., 2009b; Twomey et al., 2013), aggregate and even denature irreversibly. We therefore propose the uniform distribution of the cryoprotectant agent and the macromolecule in a frozen medium as one of the important parameters for ensuring successful stabilization and storage. We have developed **CFRM** as a method to help explore this hypothesis in a systematic manner.

Many of the bands in the Raman spectra that can be used to measure the abundance of albumin and trehalose are relatively small at low excipient concentrations, requiring a longer integration time, resulting in significant localized heating. However, albumin and trehalose generate very strong ν -CH bands. These bands were selected for the spectral analysis to minimize heating. The total organic material (albumin + trehalose) concentration in the solution and the frozen medium was determined by the ratio of the baseline-corrected integrated area of the overlapping ν -CH bands of trehalose and albumin (2820–3030 cm^{-1}) (Caspers et al., 2001; Huizinga et al., 1989; Lerbret et al., 2005; Li-Chan, 2007) to the intensity of the ν -OH band located at 3390 cm^{-1} measured with respect to a baseline along 2600–3800 cm^{-1} (Figure S1). The 3390 cm^{-1} band primarily originates from water with a very small contribution from trehalose (Branca et al., 1999; Lerbret et al., 2005; Scherer et al., 1974). Ice concentration was determined using the ratio of the integrated 3100–3200 cm^{-1} band to the intensity of the water band at 3390 cm^{-1} . The shapes and intensities of the ν -CH band are concentration and temperature dependent, requiring careful calibration. Therefore, the change in the ratio of the integrated ν -CH area to ν -OH intensity, α was plotted with respect to the concentration of trehalose and twice the concentration of albumin at 0, –5, –10, –15, and –20°C. For clarity, only the calibration curves obtained for 0 and –20°C are shown here (Figure 3) and the very small standard deviations are omitted from the figure. The calibration results showed that there was a linear correlation between α and the organic material concentration within the temperature range used in this study.

The mass ratio of albumin to trehalose was determined using the ratio of the peak intensity measured at 2935 cm^{-1} (originating primarily from albumin) (Dàvila et al., 2006) to that at 2915 cm^{-1} (originating from albumin and trehalose) (Abbate et al., 1991; Lerbret et al., 2005). The intensities of the peaks were calculated with respect to the 2880–3010 cm^{-1} baseline (Figure S2.A) for **FCL** regions with low total organic matter concentration (corresponding to less than 20 wt% trehalose), and with respect to the 2890–2990 cm^{-1} baseline (Figure S2.B) for the **FCL** regions with higher total organic matter concentration (corresponding to about 20 wt% trehalose or greater). The change in the reference baselines used to calculate intensity was made to enhance the signal to noise ratio with changing trehalose and albumin concentration and was necessitated by the dominant contribution of albumin to the ν -CH band. The change in the ratio of the peak intensity at 2935 cm^{-1} to 2915 cm^{-1} , σ , as a function of the mass ratio of albumin to trehalose was measured in the experimental range of temperatures (Figures 3B, C). These calibrations showed that the correlations between the mass ratio and σ were linear and, α and σ could therefore be used to accurately calculate the concentrations of albumin and trehalose from the Raman spectra collected from the **FCL** regions in the frozen medium.

3.2. Quantification of Microheterogeneity (MH)

The Raman spectral maps acquired in a single directional freezing experiment can be used to determine a number of parameters such as the ice crystal size and distribution, microheterogeneity, **MH**, (Figure 1), and potentially (when the S/N ratio is sufficiently high) the structural changes experienced by the macromolecules as a function of the ice growth temperature. The target data one wishes to extract from the frozen solution affects the manner in which the Raman spectral maps are collected and processed. Higher spectral and spatial resolutions require higher integration times, which inevitably causes localized heating, altering the temperature and the thermodynamic characteristics of the target region within the frozen medium. Therefore, the effects of increasing the integration time to increase the signal quality and as a result, causing higher local heating should be carefully balanced in any Raman measurement. In this study, we limited the integration time to a minimum ($t = 0.05$ s) to minimize local heating, compromising our ability to obtain macromolecular structural information. The spectral features that provide structural information are generally very subtle and would require longer integration times to increase the S/N ratio. We focused our efforts on evaluating **MH** (spatial variation in the ratio of the model protein to the cryoprotectant) in the **FCL** phase.

The degree of supercooling increased with proximity to the low temperature reservoir. This resulted in the formation of very small ice crystals surrounded by very small **FCL** regions. As a result, to be able to accurately measure **MH**, it was important to maintain the spatial resolution at the sub-micron scale while processing the spectra. Between 9 and 14 confocal Raman maps (along the microchannel starting from the low temperature reservoir, moving towards the high temperature reservoir and stopping short of the interface) were taken in each experiment, resulting in 72,000 – 112,000 spectra. Each map was collected over an area of $83.60 \mu\text{m} \times 4.032 \mu\text{m}$, and was composed of 400×20 individual spectra collected from pixels measuring $209.0 \text{ nm} \times 201.6 \text{ nm}$. To improve the S/N ratio, spectra from four neighboring pixels were averaged before the analysis.

The spatial resolution of the confocal Raman system used here was limited to a minimum voxel size of $0.4 \mu\text{m} \times 0.4 \mu\text{m} \times 0.8 \mu\text{m}$. However, the structural features within the frozen medium could be much smaller. The area corresponding to a voxel might be composed of ice or **FCL** only, or might be a mixture of **FCL** and the ice phases. Finer structural features were mainly observed in the regions with high degree of supercooling, closer to the low temperature block. Therefore, we introduced the concept of trehalose equivalent (**TE**) concentration to describe the different regions. Low **TE** concentration values served as a proxy to indicate that there were large amounts of ice in the scanned area. Conversely, scanned areas with high **TE** concentration were taken to be composed of primarily **FCL** with little or no ice present. The accuracy of the trehalose concentration and albumin/trehalose ratio measurements diminished in very low excipient concentration regions due to poor S/N ratio. To avoid biasing the results by including these areas with weak S/N, the areas with **TE** < 10 wt% were filtered out and excluded from further analysis. Likewise, areas where the calculated mass ratio of albumin/trehalose differed from the nominal value by more than a factor of three (i.e. $\sigma > 3$) were considered spurious and excluded from analysis. **TE** concentration ranges were lumped at 5% intervals (e.g., 10 wt% < **TE** < 15 wt%)

to further increase the S/N ratio (Figure 4). Furthermore, to be included in the plot, a minimum of 2% of the values at a given temperature had to fall within the **TE** range, so that only the data representing the mean of at least 40 data points were included in the plot. Mass balance analysis revealed that this exclusion did not affect the measurements conducted in the 20% and 30% trehalose solutions. However, the 10% solutions were significantly affected and were removed from the final analysis of **MH** as will be discussed later.

In all of the experiments conducted, the moving ice interface was mainly non-planar (except for a very small region within 100–200 μm of the location corresponding to the equilibrium melting temperature of the solution, where the interface stopped). Mostly, the ice interface grew in a cellular and/or dendritic pattern, generating **FCL** channels surrounded by the ice phase (Figure 2A). The non-planar growth of the ice interface was expected because of the high interface speed recorded (Figure 2C), the large thermal gradient imposed (Figure 2B), and the high viscosity of the solution (e.g. supercooled 30 wt% trehalose solution has ten times the viscosity of water at -20°C (Uchida et al., 2009)). Note that the speed of ice growth was faster in lower concentration solutions (Figure 2C). As seen in the high-resolution spectral maps included at the bottom of Figure 1 and in Figure 2A, a large variation in ice crystal and **FCL** phase morphology and distribution could be observed along the microchannel, corresponding to different temperatures. The relative intensity of the ice phase measured was inversely correlated to the trehalose concentration measured at the same location in all experiments, indicating that the identification algorithm developed was accurate.

In Figure 4, the variation of albumin to trehalose ratio in **FCL** regions with different trehalose concentrations are presented. The way data are presented in Figure 4 is quite unconventional and thus requires explanation. In Figure 4C, for example, the data show that a 20 wt% trehalose + 3 wt% albumin solution frozen at $T_F = -7.2^\circ\text{C}$ (averaged over $-7.5 < T_F < -6.9^\circ\text{C}$), contained different regions where trehalose and albumin concentrations varied significantly (showing a higher degree of **MH**). In this frozen solution, the regions that had 10–15% **TE** concentration had approximately 50% more albumin to trehalose ratio than the mean, and the regions with 25–30% **TE** concentration had approximately 5% more albumin to trehalose ratio than the mean, whereas the 20–25% **TE** and the $>30\%$ **TE** regions had approximately 5% and 10% less albumin to trehalose ratio, respectively than the mean. This indicated that in the former two regions, more albumin was present than the trehalose, potentially decreasing the protective effectiveness of trehalose, when compared to the latter two regions, which could be better protected - so long as the cryoprotectant did not crystallize. Crystallization potential depends on the type of cryoprotectant used, temperature, presence of other excipients such as salts, etc., so it is not trivial to reach a definitive conclusion. This observation is independent of the mechanism of protection offered by trehalose (whether it is by preferential exclusion (Arakawa and Timasheff, 1982) or water replacement (Clegg et al., 1982)) but indicates that the cryo-/lyoprotectant and the protein should be physically very close to one another for better protection. However, the bottom line is that the “best protocol that causes minimum **MH** within the frozen sample” would then be the one that generated a frozen medium of minimum variation from the mean albumin/trehalose ratio. For example, the same 20 wt% trehalose + 3 wt% albumin solution

frozen at 12°C showed almost no variation of albumin/trehalose ratio among different regions in the frozen medium (Figure 4C), indicating a homogeneously frozen specimen.

Some noticeable trends can be seen in Figure 4. With few exceptions, the lowest equivalent trehalose concentration range, 10–15 wt%, had an albumin/trehalose ratio higher than the mean value. Likewise, the highest equivalent trehalose concentration range (comprised of the least amount of ice), 30 wt% and greater, had an albumin/trehalose ratio that was equal to or less than the mean value in all experiments (and more pronounced at high freezing temperatures). Between these two extremes, there was a general trend of decreasing albumin/trehalose ratios in higher **TE** concentration regions. Notably, the variation in the albumin/trehalose ratio was more pronounced in the higher concentration trehalose experiments (20 wt% and 30 wt%) than in the lower concentration trehalose experiments (10 wt%).

Interestingly, the heterogeneity of the albumin distribution in the **FCL**, as evidenced by the varying albumin/trehalose ratio with respect to the **TE** concentration, was the greatest at warmer temperatures and at higher trehalose concentrations. Both of these conditions resulted in slower ice growth generating larger **FCL** regions, with lower ice contact surface. The fact that under these conditions the albumin was disproportionately distributed in areas of lower trehalose concentration and higher ice concentration could have multiple explanations. It could be the result of a bias introduced in the Raman spectra by the ice peak, which might have altered the baseline used to calculate the albumin/trehalose ratio. This explanation does not seem likely, however, since a bias introduced by the ice peak should be greatest at the lower temperatures with the greatest amount of ice. This was not the case. Another explanation could be an increase in the diffusion length scale with the larger freeze-concentrated regions, combined with the reduced mobility of the albumin in high concentration trehalose solution. Lastly, it could be the result of the affinity of the albumin for the ice surface, as has been shown to occur in dimethyl sulfoxide solutions during slow, quasi-equilibrium freezing (Twomey et al., 2013). A high affinity for the ice surface has been shown for anti-freeze proteins (Nutt and Smith, 2008; Raymond and DeVries, 1977).

In solutions that contained 10 wt% trehalose, the freezing temperature of the solution seemed to have minimal effect on the heterogeneity of the frozen system (Figure 4A, B). However, heterogeneity in the frozen medium increased with increasing amount of trehalose in the solution. This result was not terribly surprising given that the viscosity of the solution was increased and its freezing temperature was decreased with increasing amounts of trehalose in the solution. For example, in solutions that had 20 wt% trehalose, relatively uniform distribution of albumin/trehalose ratio could only be reached if the solution was frozen at $T_F < -14$ °C (Figure 4C, D). Higher freezing temperatures created regions of high (as high as 150% of the mean) albumin/trehalose ratio as well as regions of low (as low as 40% of the mean) albumin/trehalose ratio. In the high ratio regions, protection offered by trehalose could decrease and albumin aggregation, and potentially denaturation could increase significantly. On the contrary, in the low ratio regions, the presence of excess trehalose might cause crystallization during storage. Also in high trehalose concentration protein solutions (30 wt% ~ 0.1M), freezing the model solution at a relatively high supercooling level (-14 °C $< T_F < -12$ °C) resulted in a relatively homogeneous distribution

of albumin/trehalose ratio, increasing the likelihood that trehalose and albumin will co-localize and the protein will thus be protected from the adverse effects of exposure to the ice interface. At higher subzero temperatures ($-6\text{ }^{\circ}\text{C} < T_F < -2\text{ }^{\circ}\text{C}$), on the other hand, regions of significantly variable albumin/trehalose ratio (ranging from 140% of the mean down to 80% of the mean) was observed. This pointed at insufficient protection for albumin.

Figure 5 shows the absolute microheterogeneity (**MH**) in the samples experimented with as a function of freezing temperature. Note that the lines in the plot are only guides for the eye and the 10% trehalose solutions were excluded from the plot due to failure of these experiments to satisfy the mass balance check. **MH** was calculated using Equation 1 presented below where $(R_{A/T})_i$ is the albumin to trehalose ratio measured in each **TE** region within a medium at a specific freezing temperature, T_F , and f_i is the respective concentration frequency (percentage of albumin in the whole solution that was found in that **TE** range).

$$MH = \sum_{i=10\%}^{i=30\%} Abs[(R_{A/T})_i - 100] * f_i \quad (1)$$

With reducing temperatures (and increasing supercooling) and increasing trehalose concentration in the solution, the mobility of the excipients in the solution are expected to decrease due to increase in the viscosity. In the meantime, the ice propagation speed increases (Figure 2C) due to freezing becoming thermodynamically more favorable. This would then indicate that more solutes would be engulfed by the ice in a smaller volume, and possibly reach higher concentrations. Our results presented in Figure 5 showed that the freezing temperature was a very significant factor in determining the distribution of the model protein and cryo/lyo-protectant within the solution. The **MH** in the frozen solution decreased very significantly below $-10\text{ }^{\circ}\text{C}$, indicating that a much more uniformly frozen solution could be obtained if freezing was achieved at lower cryogenic temperatures.

It should be emphasized here that the low S/N ratio spectra collected in this study to minimize localized heating has resulted in large variation in the calibration experiments (Figure 3). This implies that the results presented in Figure 4 have to be interpreted with caution and the variation in the data has to be noted. However, the effect of this on the main observation in this paper as presented in Figure 5 is expected to be minimum.

4. SUMMARY

The morphology, final composition, and **MH** within a frozen product is influenced by many factors, including the initial composition of the aqueous solution (Dong et al., 2009b; Sei et al., 2002; Twomey et al., 2013; Zhang et al., 2005), and the freezing conditions (degree of supercooling, pre-freeze cooling rate, freezing temperature, and post-freeze cooling rate) (Petzold and Aguilera, 2009). A thorough analysis of all combinations of parameters requires thousands of experiments to be run, which is costly, time consuming and prone to error. Therefore, in this communication we introduced a novel method (**CFRM**) that can be further developed to be used in screening of the developed formulations and/or the freezing protocols very rapidly, using a few experiments. We envision that the methodology will also

find widespread use in other fields, such as in food science where preservation and stabilization is of utmost importance.

Initial results obtained with **CFRM** from experiments conducted with albumin and trehalose indicates that there was heterogeneity in the distribution of the protein in the freeze-concentrated liquid, and that the protein is preferentially distributed near the ice phase. Analysis of the absolute **MH** in the frozen solutions showed that high degree of supercooling before freezing was beneficial to reduce the spatial variation within the frozen product.

Supplementary Material

Refer to Web version on PubMed Central for supplementary material.

ACKNOWLEDGEMENTS

This research was partially funded by an NSF grant (1335936) to AA, a Japan Society for the Promotion of Science (JSPS) fellowship to AA, an NIH-NCI grant (1R21CA157298-01A1) to AA, and an NSF-EAPSI/JSPS Summer Fellowship to AT. The authors thank the anonymous reviews whose constructive critiques have significantly improved this manuscript.

REFERENCES

- Abbate S, Conti G, Naggi A. Characterisation of the glycosidic linkage by infrared and Raman spectroscopy in the C-H stretching region: α,α -trehalose and α,α -trehalose-2,3,4,6,6-d10. 1991; 210:1–12.
- Aksan, A.; Toner, M. Role of thermodynamic state and molecular mobility in biopreservation. In: Bronzino, JD., editor. Tissue Engineering and Artificial Organs. Taylor & Francis, Boca Raton, FL: 2006. p. 41.41-41.20.
- Arakawa T, Timasheff SN. Stabilization of Protein Structure by Sugars. Biochemistry. 1982; 21:6536–6544. [PubMed: 7150574]
- Basi S, Lewis JB. Microalbuminuria as a target to improve cardiovascular and renal outcomes. American journal of kidney diseases: the official journal of the National Kidney Foundation. 2006; 47:927. [PubMed: 16731288]
- Bhatnagar BS, Bogner RH, Pikal MJ. Protein Stability During Freezing: Separation of Stresses and Mechanisms of Protein Stabilization. Pharmaceutical Development and Technology. 2007; 12:505–523. [PubMed: 17963151]
- Bhattacharya AA, Grüne T, Curry S. Crystallographic analysis reveals common modes of binding of medium and long-chain fatty acids to human serum albumin. Journal of molecular biology. 2000; 303:721. [PubMed: 11061971]
- Branca C, Magazù S, Maisano G, Migliardo P. Anomalous cryoprotective effectiveness of trehalose: Raman scattering evidences. The Journal of chemical physics. 1999; 111:281.
- Butler MF. Freeze Concentration of Solutes at the Ice/Solution Interface Studied by Optical Interferometry. Crystal Growth & Design. 2002; 2:541–548.
- Carpenter, JF.; Chang, BS. Lyophilization of Protein Pharmaceuticals. In: Avis, K.; Wu, V., editors. Biotechnology and Biopharmaceutical Manufacturing, Processing and Preservation. Buffalo Grove, IN: Interpharm Press; 1996.
- Carpenter JF, Crowe JH. An Infrared Spectroscopic Study of the Interactions of Carbohydrates with Dried Proteins. Biochemistry. 1989; 28:3916–3922. [PubMed: 2526652]
- Carpenter JF, Crowe JH, Arakawa T. Comparison of Solute-Induced Protein Stabilization in Aqueous Solution and in the Frozen and Dried States. Journal of Dairy Science. 1990; 73:3627–3636.

- Caspers PJ, Lucassen GW, Carter EA, Bruining HA, Puppels GJ. In vivo confocal Raman microspectroscopy of the skin: noninvasive determination of molecular concentration profiles. *Journal of investigative dermatology*. 2001; 116:434–442. [PubMed: 11231318]
- Cavatur RK, Suryanarayanan R. Characterization of frozen aqueous solutions by low temperature X-ray powder diffractometry. *Pharmaceutical Research*. 1998; 15:194–199. [PubMed: 9523303]
- Cavatur RK, Vemuri NM, Pyne A, Chrzan Z, Toledo-Velasquez D, Suryanarayanan R. Crystallization behavior of mannitol in frozen aqueous solutions. *Pharmaceutical Research*. 2002; 19:894–900. [PubMed: 12134963]
- Chang L, Shepherd D, Sun J, Ouellett D, Grant KL, Tang X, Pikal MJ. Mechanism of protein stabilization by sugars during freeze-drying and storage: Native structure preservation, specific interaction, and/or immobilization in a glassy matrix. *Journal of Pharmaceutical Sciences*. 2005; 94:1427–1444. [PubMed: 15920775]
- Clegg JS, Seitz P, Seitz W, Hazlewood CF. Cellular Response to Extreme Water Loss: The Water-Replacement Hypothesis. *Cryobiology*. 1982; 19:306–316. [PubMed: 7105783]
- Crowe JH, Anchordoguy TJ, Carpenter JF, Loomis SH, Crowe LM. Interactions of Natural Cryoprotectants with Membranes and Proteins. *Cryobiology*. 1988; 25:556–556.
- Crowe JH, Carpenter JF, Crowe LM, Anchordoguy TJ. Are Freezing and Dehydration Similar Stress Vectors - a Comparison of Modes of Interaction of Stabilizing Solutes with Biomolecules. *Cryobiology*. 1990; 27:219–231.
- Cuffey KM, Conway H, Hallet B, Gades AM, Raymond CF. Interfacial water in polar glaciers and glacier sliding at –17 C. *Geophysical Research Letters*. 1999; 26:751–754.
- Dàvila E, Parés D, Howell NK. Fourier transform raman spectroscopy study of heat-induced gelation of plasma proteins as influenced by pH. *Journal of agricultural and food chemistry*. 2006; 54:7890–7897. [PubMed: 17002467]
- Dong J, Hubel A, Bischof JC, Aksan A. Freezing-Induced Phase Separation and Spatial Microheterogeneity in Protein Solutions. *J. Phys. Chem. B*. 2009a; 113:10081–10087. [PubMed: 19580250]
- Dong J, Hubel A, Bischof JC, Aksan A. Freezing-Induced Phase Separation and Spatial Microheterogeneity in Protein Solutions. *The Journal of Physical Chemistry B*. 2009b; 113:10081–10087. [PubMed: 19580250]
- Eckhardt B, Oeswein J, Bewley T. Effect of Freezing on Aggregation of Human Growth Hormone. *Pharmaceutical Research*. 1991a; 8:1360–1364. [PubMed: 1798670]
- Eckhardt BM, Oeswein JQ, Bewley TA. Effect of Freezing on Aggregation of Human Growth Hormone. *Pharmaceutical Research*. 1991b; 8:1360–1364. [PubMed: 1798670]
- Fradkin AH, Carpenter JF, Randolph TW. Immunogenicity of aggregates of recombinant human growth hormone in mouse models. *J Pharm Sci*. 2009; 98:3247–3264. [PubMed: 19569057]
- Gekle M. Renal tubule albumin transport. *Annu. Rev. Physiol*. 2005; 67:573–594. [PubMed: 15709971]
- Heller MC, Carpenter JF, Randolph TW. Effects of Phase Separating Systems on Lyophilized Hemoglobin. *Journal of Pharmaceutical Sciences*. 1996; 85:1358–1362. [PubMed: 8961153]
- Heller MC, Carpenter JF, Randolph TW. Manipulation of Lyophilization-Induced Phase Separation: Implications for Pharmaceutical Proteins. *Biotechnology Progress*. 1997; 13:590–596. [PubMed: 9336978]
- Heller MC, Carpenter JF, Randolph TW. Application of a Thermodynamic Model to the Prediction of Phase Separations in Freeze-Concentrated Formulations for Protein Lyophilization. *Archives of Biochemistry and Biophysics*. 1999a; 363:191–201. [PubMed: 10068440]
- Heller MC, Carpenter JF, Randolph TW. Protein Formulation and Lyophilization Cycle Design: Prevention of Damage Due to Freeze-Concentration Induced Phase Separation. *Biotechnol. Bioeng*. 1999b; 63:166–174. [PubMed: 10099593]
- Hew CL, Yang DSC. PROTEIN-INTERACTION WITH ICE. *Eur. J. Biochem*. 1992; 203:33–42. [PubMed: 1730239]
- Hobbs, PV. *Ice physics*. Oxford: Clarendon Press; 1974. 1974 1.
- Hubel A, Aksan A, Skubitz APN, Wendt C, Zhong X. State of the Art in Preservation of Fluid Biospecimens. *Biopreserv. Biobank*. 2011; 9:237–244. [PubMed: 24850337]

- Huizinga A, Bot ACC, de Mul FFM, Vrensen GFJM, Greve J. Local variation in absolute water content of human and rabbit eye lenses measured by Raman microspectroscopy. 1989; 48:487–496.
- Izutsu K, Kojima S. Freeze-concentration separates proteins and polymer excipients into different amorphous phases. *Pharmaceutical Research*. 2000; 17:1316–1322. [PubMed: 11145240]
- Jovanovic N, Gerich A, Bouchard A, Jiskoot W. Near-infrared imaging for studying homogeneity of protein-sugar mixtures. *Pharmaceutical Research*. 2006; 23:2002–2013. [PubMed: 16906457]
- Kawai K, Suzuki T. Stabilizing Effect of Four Types of Disaccharide on the Enzymatic Activity of Freeze-dried Lactate Dehydrogenase: Step by Step Evaluation from Freezing to Storage. *Pharmaceutical Research*. 2007; 24:1883–1890. [PubMed: 17486434]
- Kerwin BA, Heller MC, Levin SH, Randolph TW. Effects of tween 80 and sucrose on acute short-term stability and long-term storage at –20 °C of a recombinant hemoglobin. 1998; 87:1062–1068.
- Klajnert B, Bryszewska M. Fluorescence studies on PAMAM dendrimers interactions with bovine serum albumin. *Bioelectrochemistry*. 2002; 55:33–35. [PubMed: 11786335]
- Korber C. Phenomena at the advancing ice-liquid interface: solutes, particles and biological cells. *Q Rev Biophys*. 1988; 21:229–298. [PubMed: 3043537]
- Korber C, Scheiwe M, Wollhover K. Observations on the non-planar freezing of aqueous salt solutions. *J. Crystal Growth*. 1983; 61:307–316.
- Langer JS. INSTABILITIES AND PATTERN-FORMATION IN CRYSTAL-GROWTH. *Rev. Mod. Phys*. 1980; 52:1–28.
- Lerbret A, Bordat P, Affouard F, Guinet Y, Hédoux A, Paccou L, Prévost D, Descamps M. Influence of homologous disaccharides on the hydrogen-bond network of water: complementary Raman scattering experiments and molecular dynamics simulations. Conformations of Oligo- and Polysaccharides. 2005; 340:881–887.
- Leslie SB, Israeli E, Lighthart B, Crowe JH, Crowe LM. Trehalose and sucrose protect both membranes and proteins in intact bacteria during drying. *Applied and Environmental Microbiology*. 1995; 61:3592–3597. [PubMed: 7486995]
- Li-Chan ECY. Vibrational spectroscopy applied to the study of milk proteins. *Le Lait*. 2007; 87:443–458.
- Lins RD, Pereira CS, Hünenberger PH. Trehalose–protein interaction in aqueous solution. *Proteins: Structure, Function, and Bioinformatics*. 2004; 55:177–186.
- Lipp G, Körber C. On the engulfment of spherical particles by a moving ice-liquid interface. *J. Cryst. Growth*. 1993; 130:475–489.
- McLerran D, Grizzle W, Feng Z, Bigbee W, Banez L, Cazares L. Analytical validation of serum proteomic profiling for diagnosis of prostate cancer; sources of sample bias. *Clinical Chemistry*. 2008a; 54:44–52. [PubMed: 17981926]
- McLerran D, Grizzle WE, Feng Z, Bigbee WL, Banez LL, Cazares LH, Chan DW, Diaz J, Izbicka E, Kagan J. Analytical validation of serum proteomic profiling for diagnosis of prostate cancer: sources of sample bias. *Clinical chemistry*. 2008b; 54:44–52. [PubMed: 17981926]
- McLerran D, Grizzle WE, Feng Z, Bigbee WL, Banez LL, Cazares LH, Chan DW, Diaz J, Izbicka E, Kagan J, Malehorn DE, Malik G, Oelschlager D, Partin A, Randolph T, Rosenzweig N, Srivastava S, Srivastava S, Thompson IM, Thornquist M, Troyer D, Yasui Y, Zhang Z, Zhu L, Semmes OJ. Analytical validation of serum proteomic profiling for diagnosis of prostate cancer: Sources of sample bias. *Clinical Chemistry*. 2008c; 54:44–52. [PubMed: 17981926]
- Murase N, Echlin P, Franks F. The Structural States of Freeze-Concentrated and Freeze-Dried Phosphates Studied by Scanning Electron Microscopy and Differential Scanning Calorimetry. *Cryobiology*. 1991; 28:364–375.
- Murase N, Franks F. Salt Precipitation During the Freeze-Concentration of Phosphate Buffer Solutions. *Biophysical Chemistry*. 1989; 34:293–300. [PubMed: 2611352]
- Nagashima K, Furukawa Y. Solute distribution in front of an ice/water interface during directional growth of ice crystals and its relationship to interfacial patterns. *J. Phys. Chem. B*. 1997; 101:6174–6176.

- Nutt DR, Smith JC. Dual Function of the Hydration Layer around an Antifreeze Protein Revealed by Atomistic Molecular Dynamics Simulations. *Journal of the American Chemical Society*. 2008; 130:13066–13073. [PubMed: 18774821]
- Padilla AM, Pikal MJ. The Study of Phase Separation in Amorphous Freeze-Dried Systems, Part 2: Investigation of Raman Mapping as a Tool for Studying Amorphous Phase Separation in Freeze-Dried Protein Formulations. *Journal of Pharmaceutical Sciences*. 2011; 100:1467–1474. [PubMed: 20967837]
- Pardridge WM. Plasma protein-mediated transport of steroid and thyroid hormones. *American Journal of Physiology-Endocrinology And Metabolism*. 1987; 252:E157–E164.
- Pardridge WM, Mietus LJ. Transport of steroid hormones through the rat blood-brain barrier: primary role of albumin-bound hormone. *Journal of Clinical Investigation*. 1979; 64:145. [PubMed: 447850]
- Peakman TC, Elliott P. The UK Biobank sample handling and storage validation studies. *International journal of epidemiology*. 2008; 37:i2–i6. [PubMed: 18381389]
- Petzold G, Aguilera JM. Ice morphology: fundamentals and technological applications in foods. *Food Biophysics*. 2009; 4:378–396.
- Piedmonte D, Summers C, McAuley A, Karamujic L, Ratnaswamy G. Sorbitol Crystallization Can Lead to Protein Aggregation in Frozen Protein Formulations. *Pharmaceutical Research*. 2007; 24:136–146. [PubMed: 17109212]
- Pikal, MJ. Freeze-Drying of Proteins. In: Cleland, JL.; Langer, R., editors. *Stability, Formulation and Delivery of Peptides and Proteins*. Washington, DC: American Chemical Society; 1994. p. 120-133.
- Ragoonanan V, Aksan A. Protein stabilization. *Transfusion Medicine and Hemotherapy*. 2007; 34:246–252.
- Ragoonanan V, Aksan A. Heterogeneity in Desiccated Solutions: Implications for Biostabilization. *Biophysical Journal*. 2008; 94:2212–2227. [PubMed: 18055531]
- Randolph TW. Phase separation of excipients during lyophilization: Effects on protein stability. *Journal of Pharmaceutical Sciences*. 1997; 86:1198–1203. [PubMed: 9383725]
- Randolph TW, Carpenter JF. Engineering Challenges of Protein Formulations. *AIChE Journal*. 2007; 53:1902–1907.
- Rathore N, Rajan RS. Current Perspectives on Stability of Protein Drug Products during Formulation, Fill and Finish Operations. *Biotechnology Progress*. 2008; 24:504–514. [PubMed: 18484778]
- Raymond JA, DeVries AL. Adsorption inhibition as a mechanism of freezing resistance in polar fishes. *Proceedings of the National Academy of Sciences*. 1977; 74:2589.
- Remmele RL, Stushnoff C. Low-Temperature IR Spectroscopy Reveals Four Stages of Water Loss During Lyophilization of Hen Egg White Lysozyme. *Biopolymers*. 1994; 34:365–370.
- Riegman PHJ, Morente MM, Betsou F, de Blasio P, Geary P. Biobanking for better healthcare. 2008; 2:213–222.
- Scherer JR, Go MK, Kint S. Raman spectra and structure of water from –10 to 90.deg. *The Journal of Physical Chemistry*. 1974; 78:1304–1313.
- Schwegman JJ, Carpenter JF, Nail SL. Evidence of partial unfolding of proteins at the ice/freeze-concentrate interface by infrared microscopy. *Journal of Pharmaceutical Sciences*. 2009; 98:3239–3246. [PubMed: 19544369]
- Sei T, Gonda T, Arima Y. Growth rate and morphology of ice crystals growing in a solution of trehalose and water. *Journal of crystal growth*. 2002; 240:218–229.
- Shalaev EY, Franks F. Changes in the Physical State of Model Mixtures during Freezing and Drying: Impact on Product Quality. *Cryobiology*. 1996; 33:11–26.
- Shalaev EY, Kanev AN. Study of the Solid-Liquid State Diagram of the Water-Glycine-Sucrose System. *Cryobiology*. 1994; 31:374–382.
- Shen Y, Jacobs JM, Camp DG, Fang R, Moore RJ, Smith RD, Xiao W, Davis RW, Tompkins RG. Ultra-high-efficiency strong cation exchange LC/RPLC/MS/MS for high dynamic range characterization of the human plasma proteome. *Analytical chemistry*. 2004; 76:1134–1144. [PubMed: 14961748]

- Strambini GB, Gabellieri E. Proteins in frozen solutions: Evidence of ice-induced partial unfolding. *Biophysical Journal*. 1996; 70:971–976. [PubMed: 8789114]
- Strambini GB, Gonnelli M. Protein Stability in Ice. *Biophysical Journal*. 2007; 92:2131–2138. [PubMed: 17189314]
- Sundaramurthi P, Shalaev E, Suryanarayanan R. “pH Swing” in Frozen Solutions—Consequence of Sequential Crystallization of Buffer Components. *The Journal of Physical Chemistry Letters*. 2009; 1:265–268.
- Suzuki T, Franks F. Solid-Liquid Phase Transitions and Amorphous States in Ternary Sucrose-Glycine-Water Systems. *Journal of the Chemical Society, Faraday Transactions*. 1993; 89:3283–3288.
- Tang X, Pikal M. Design of Freeze-Drying Processes for Pharmaceuticals: Practical Advice. *Pharmaceutical Research*. 2004; 21:191–200. [PubMed: 15032301]
- Tang X, Pikal MJ. The Effect of Stabilizers and Denaturants on the Cold Denaturation Temperatures of Proteins and Implications for Freeze-Drying. *Pharmaceutical Research*. 2005; 22:1167–1175. [PubMed: 16028018]
- Twomey A, Less R, Kurata K, Takamatsu H, Aksan A. In Situ Spectroscopic Quantification of Protein–Ice Interactions. *J. Phys. Chem. B*. 2013; 117:7889–7897. [PubMed: 23742723]
- Uchida T, Nagayama M, Gohara K. Trehalose solution viscosity at low temperatures measured by dynamic light scattering method: Trehalose depresses molecular transportation for ice crystal growth. *J. Cryst. Growth*. 2009; 311:4747–4752.
- Uchida, T.; Takeya, S.; Nagayama, M.; Gohara, K. Freezing Properties of Disaccharide Solutions: Inhibition of Hexagonal Ice Crystal Growth and Formation of Cubic Ice. In: Borisenko, E., editor. *Crystallization and Materials Science of Modern Artificial and Natural Crystals*. 2012. InTech.s.
- Wolkers WF, Walker NJ, Tablin F, Crowe JH. Human platelets loaded with trehalose survive freeze-drying. *Cryobiology*. 2001; 42:79. [PubMed: 11448110]
- Zhang H, Hussain I, Brust M, Butler MF, Rannard SP, Cooper AI. Aligned two- and three-dimensional structures by directional freezing of polymers and nanoparticles. *Nature materials*. 2005; 4:787–793.
- Zimmermann J, Hajibabaei M, Blackburn DC, Hanken J, Cantin E, Posfai J, Evans TC Jr. DNA damage in preserved specimens and tissue samples: a molecular assessment. *Frontiers in Zoology*. 2008; 5:1–13. [PubMed: 18171469]

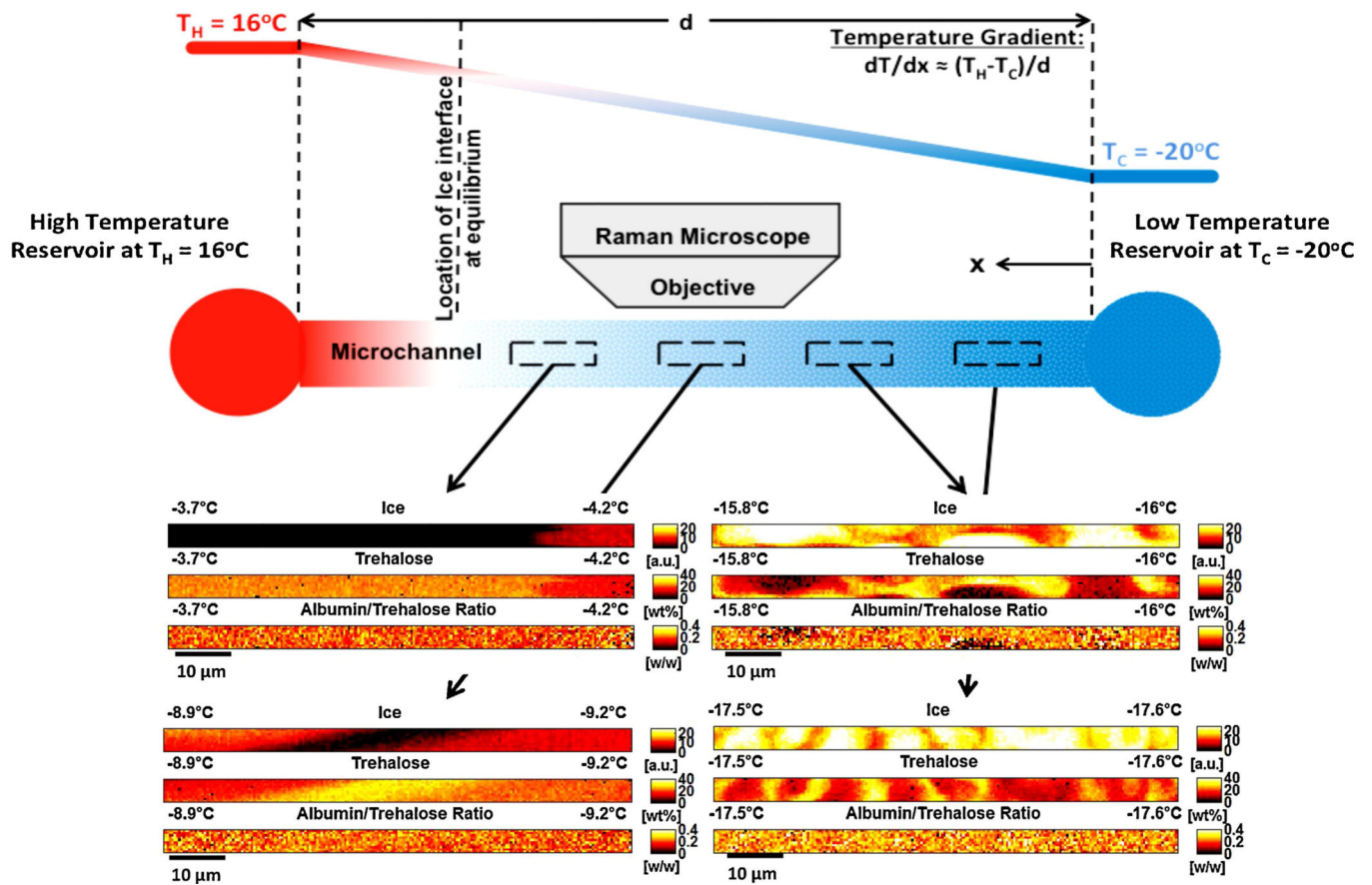
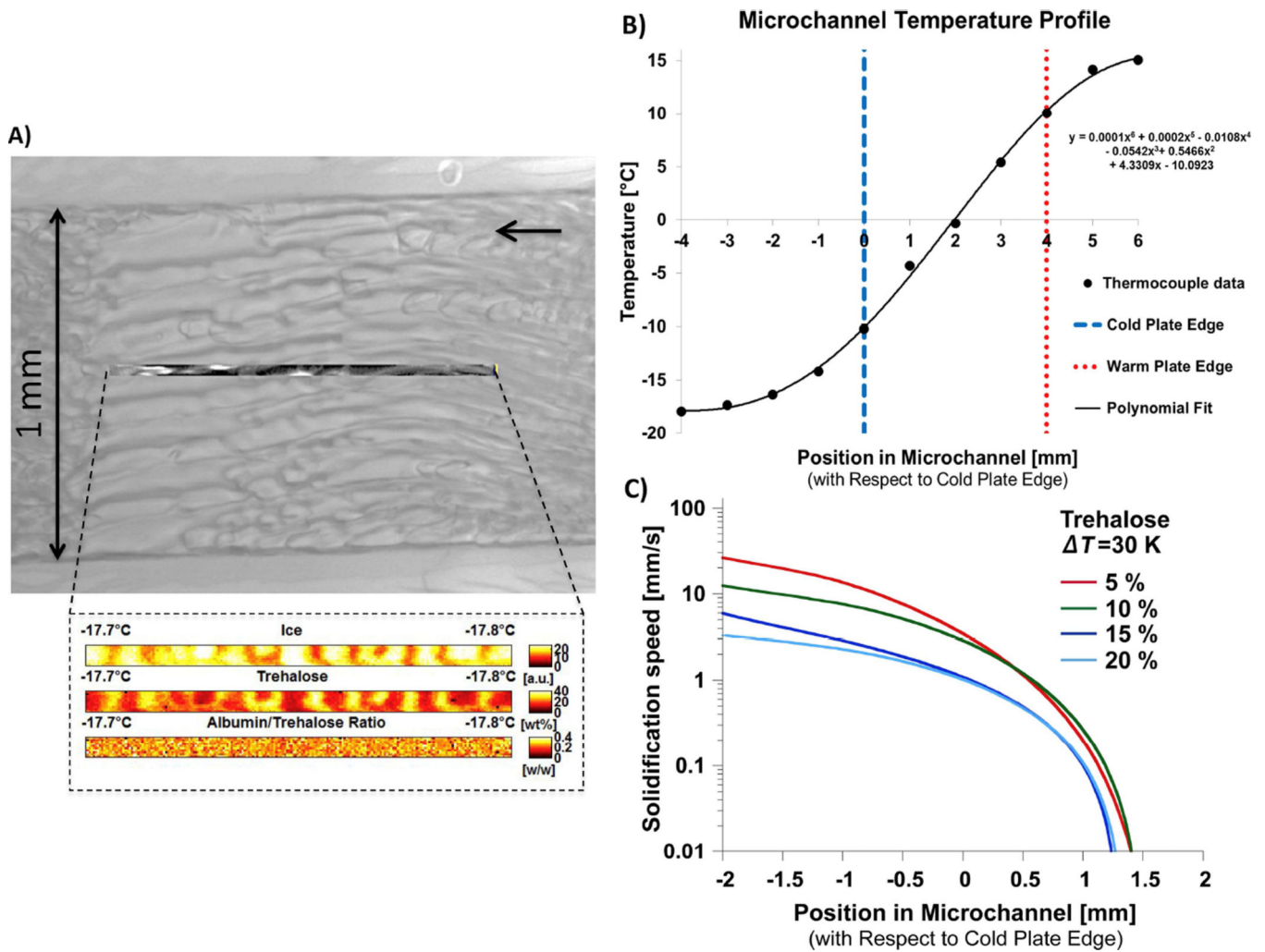


Figure 1. Schematic of the experimental setup, and representative Raman maps collected from different regions in the microchannel.



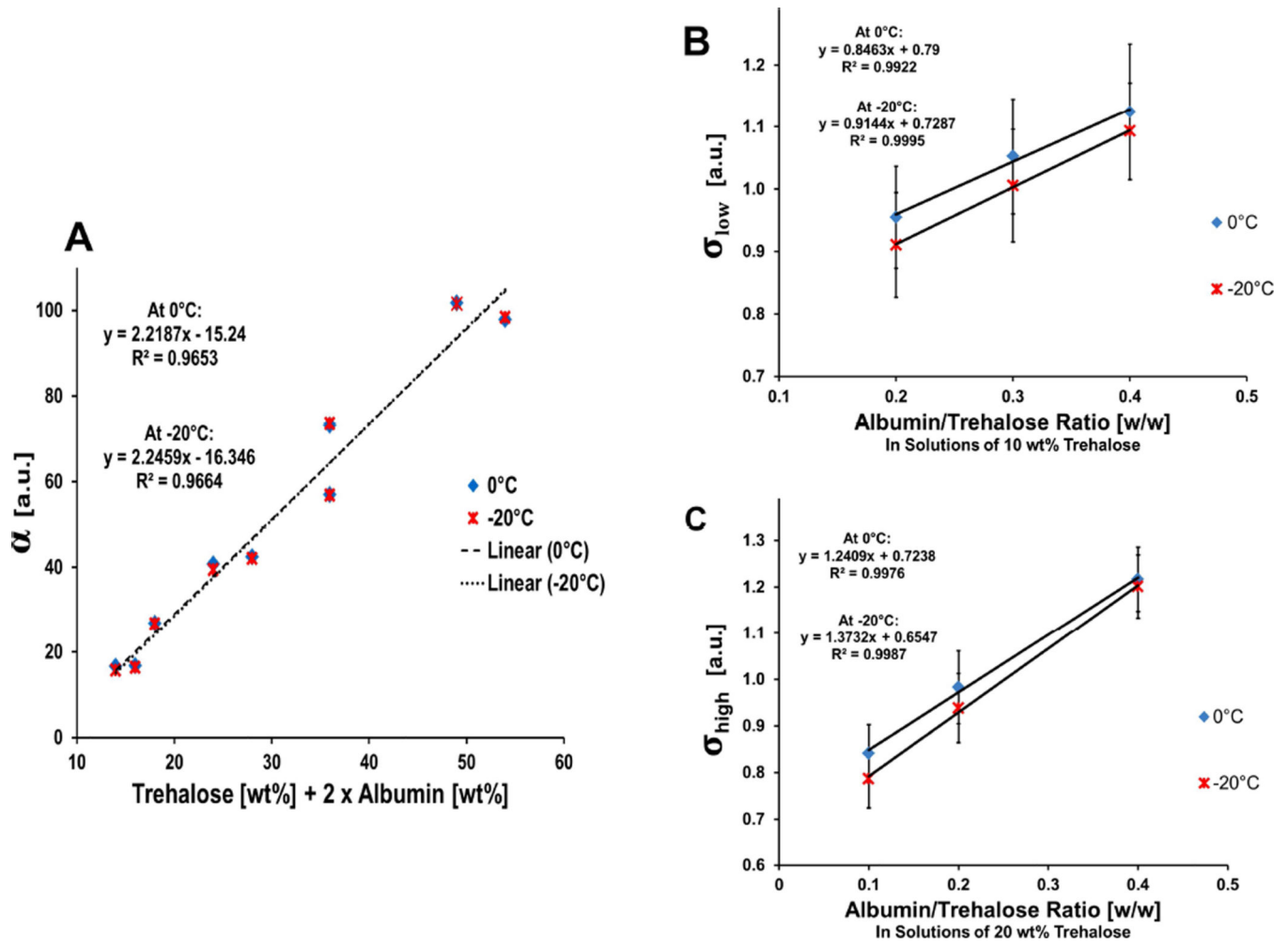


Figure 3. Spectral calibrations used to measure concentration from the collected Raman spectra. **A)** Change in the ratio of the integrated ν -CH area to ν -OH intensity (α) with trehalose and albumin concentration. Change in the ratio of the peak intensity at 2935 cm^{-1} to 2915 cm^{-1} (σ) with albumin/trehalose ratio at regions of **B)** low, **C)** high albumin concentration.

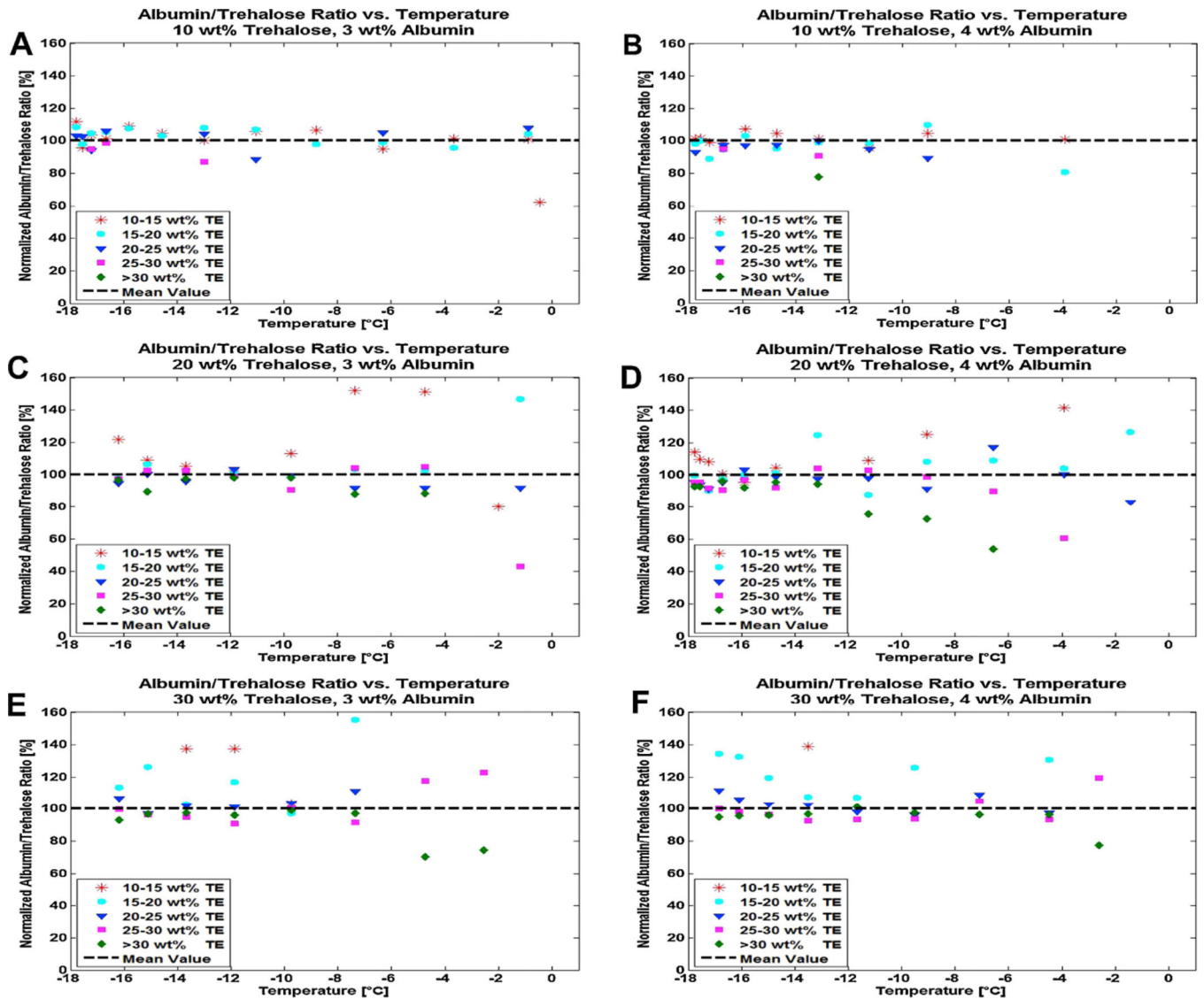


Figure 4.
Change in albumin/trehalose mass ratio in the frozen solution with freezing temperature, T_F .
A) 10 wt% trehalose and 3 wt% albumin. **B)** 10 wt% trehalose and 4 wt% albumin. **C)** 20 wt % trehalose and 3 wt% albumin. **D)** 20 wt% trehalose and 4 wt% albumin. **E)** 30 wt% trehalose and 3 wt% albumin. **F)** 30 wt% trehalose and 4 wt% albumin.

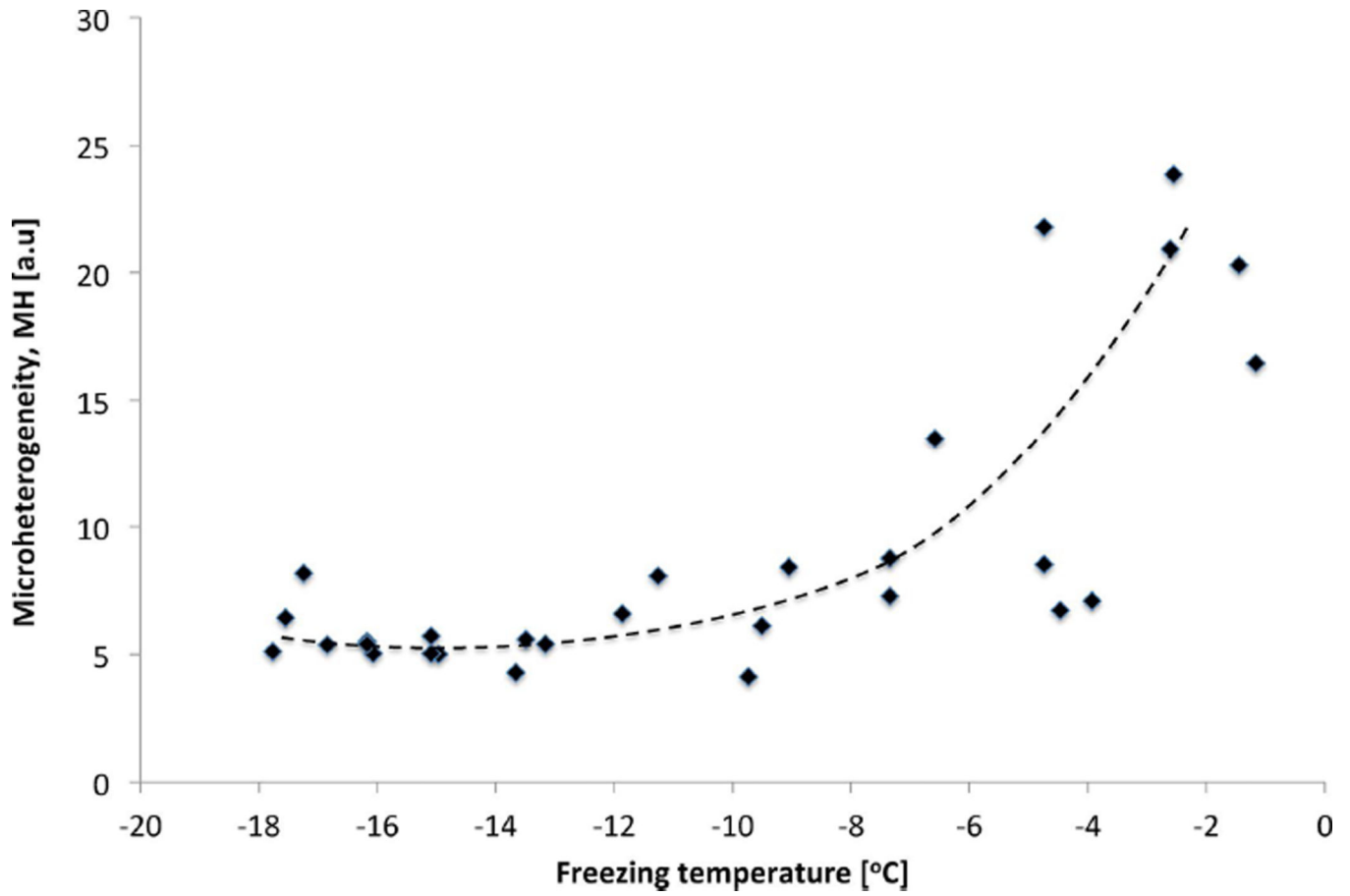


Figure 5.
Microheterogeneity (MH) as a function of freezing temperature.

Table 1

Excipient concentrations in calibration experiments conducted with 1× DPBS

Trehalose [wt%]	Albumin [wt%]	Albumin/Trehalose [w/w]
10	2	0.2
10	3	0.3
10	4	0.4
20	2	0.1
20	4	0.2
20	6	0.4
30	3	0.1
30	6	0.2
30	12	0.4
35	7	0.2

Author Manuscript

Author Manuscript

Author Manuscript

Author Manuscript

Table 2

Excipient concentrations in directional freezing experiments conducted with 1× DPBS

Trehalose [wt%]	Albumin [wt%]	Albumin/Trehalose [w/w]
10	2	0.20
10	3	0.30
10	4	0.40
20	2	0.10
20	3	0.15
20	4	0.20
30	3	0.10
30	4	0.13

Author Manuscript

Author Manuscript

Author Manuscript

Author Manuscript